

COMPUTATIONAL EVALUATION OF C-130 DRAG REDUCTION WITH AFTBODY MODIFICATIONS

Erdem Ayan¹
Middle East Technical University
Ankara, Turkey

Hakan Telli², Y. Volkan Pehlivanođlu³
Turkish Air Force Academy
Istanbul, Turkey

ABSTRACT

This paper represents the second phase of a computational study to investigate the effects of aft body modifications on the total drag of C-130E aircraft. The overall study focuses on the possible increment in fuselage form drag due to generated vortices on the underside of the highly upswept aft region. The initial phase of the study consists of computational fluid dynamics (CFD) analyses of the flowfield around the aircraft to evaluate the drag reduction performance of finlets attached on the lower surface of the aft body. As the second phase, the contribution of the microvanes on the aircraft's performance is computationally investigated and the results are compared. Microvanes are small and bumped-shaped devices installed on each side of the fuselage's aft section to reduce the drag. Various finlet and microvane configurations are created in different sizes and numbers to reduce the drag of the full aircraft. The analyses are performed by using Reynolds-averaged Navier-Stokes (RANS) with Spalart-Allmaras turbulence model. The simulations are made with flow solver ANSYS Fluent 14.0 on a high-performance Linux cluster. Considering 1 drag count as 0.0001, up to 18 counts of drag reduction is achieved with some of the finlet and microvane configurations analyzed.

I. INTRODUCTION

The Lockheed Martin C-130E is one of the most popular and widely used military transport aircrafts, which has also been used in the Turkish Air Forces since 1964. There have been several investigations so far to evaluate and improve the flight performance characteristics of the C-130. Aircraft drag-reduction research is one of the main aspects of these investigations. Military transport aircrafts, like C-130, differ from other aircrafts by rapidly decreasing fuselage cross-section due to the highly up-swept aft fuselage part. It is asymmetrically designed with a pronounced upsweep of its lower surface [Bury, Morton and Charles, 2008]. During the flight, the complex flow field is initiated with this decreasing cross-section on the lower contour of the afterbody. Subsequently, the afterbody flow field can have detailed vortex structure which is characterized by a pair of large counter-rotating vortices that convey far downstream [Epstein, Carbonaro and Caudron, 1994]. Accordingly, rear fuselage form drag due to generated vortices becomes a significant contributor of the overall aircraft drag. A reduction of that induced drag by half might represent a 5% reduction in total drag [Thomas, 1985].

In order to reduce the afterbody drag of an aircraft having highly upswept aft body, researchers have developed several techniques and investigated them. For axisymmetric bluff bodies having low fineness ratio, rather than using a gradual afterbody closure – that causes useful volume loss, large

¹ Ph.D. Student at Aerospace Engineering Department, Email: erdem.ayan@metu.edu.tr

² M.S. Student at Department of Aeronautics and Space Technologies Institute, Email: htelli@hho.edu.tr

³ Asst. Prof. in Turkish Air Force Academy, Email: v.pehlivan@hho.edu.tr

scale V-type surface grooves were used to eliminate flow separation and decrease drag by creating longitudinal and continuous vortices [Quass, Howard, Weinstein and Bushnell, 1981]. In addition to the longitudinal V-type grooving, smooth afterbodies with shoulder radiusing and circumferentially grooved afterbodies were investigated at a subsequent study [Howard and Goodman, 1985]. In another study, drag reduction potential of the vortex generators placed at some strategic points on 1/72 scale C-130 fuselage was experimentally investigated. As a result, appreciable drag reduction for some of the configurations was achieved [Calarese, Crisler and Gustafson, 1985]. 1:17 scale models of fuselages of Boeing 747 and Lockheed C-5 were used in experiments to validate that pairs of vortex generators added on the lower surface of the swept aftbody would prevent or delay separation by energizing the boundary layer and reduce the form drag. Results showed that greater gains in performance are possible on aft-loading military transports [Wortman, 1999]. As a part of the researches conducted by Lockheed Martin Aeronautics and the United States Air Force Academy to investigate various methods of drag reduction on C-130 aircraft, studies focused on the beavertail strakes attached on the aft-body of the airframe. In these experimental studies, several types of strakes were tested at some Mach numbers to evaluate the drag reduction performance of the strakes and predict the in-flight aerodynamic loads [Wooten and Yechout, 2009]. Subsequently, the drag reduction performance of the strake modification through a representative range of C-130 deck angles was investigated, and analyzed and defined the static stability changes [Pinsky, Gray, Welch and Yechout, 2009]. Based on CFD analysis and wind tunnel tests, [Mirzaei, Karimi and Vaziri, 2012] investigated the effect of upsweep angle and the cross-section contour on drag coefficient of a tactical cargo aircraft.

The rotation phase of take-off and the mission requirements, such as airdrop operations and the need of a main cargo door for prompt loading, affect the design of the military transport aircrafts. In addition, they are designed to reach larger cargo capacity. Therefore, aft section of the military transport aircrafts has higher ramp angles than the commercial aircrafts. For instance, up-sweep angle of C-130 aft fuselage is about 28° . Due to that significant ramp, the air flow sweeps around the sides of the fuselage toward the bottom, resulting in vortices that form on the underside of the aft fuselage. The vortices become stronger as they progress downstream and interact with the empennage. This results in a significant contribution to the drag of the aircraft; and so higher fuel consumption. As the number of cargo aircrafts increases in military fleets with fuel costs, the necessity to reduce the drag coefficient becomes more important. Therefore, the need to decrease the fuel consumption due to induced drag, and so to increase the performance of C-130, was motivated the present study.

Final design of most of the cargo aircrafts have been completed in the early years of 1960s. Later modifications for enhanced performance have been performed with extra add-ons on wings or fuselages. In this paper, two types of add-ons which are finlets and microvanes have been investigated to understand their drag reduction potential on cargo aircrafts. Computational Fluid Dynamics was used with RANS modeling in the analysis. The model and the method were validated with wind tunnel tests carried out earlier [Pinsky, Gray, Welch and Yechout, 2009]. Various finlet and microvane configurations have been created and examined in the design part. Different parameters have been used to reach the most efficient design. Having properly defined the size, shape and location of the add-ons it is possible to separate larger vortices into smaller ones by increasing energy capacity of the boundary layer and creating early vortices. Therefore, for both finlet and microvane studies, desired reduction in the drag coefficient of C-130 was achieved.

II. THEORY

Occurrence of flow separation is directly related to the boundary layer energy. Flow generally aims to follow a parallel lane to the wall. When the speed of the boundary layer relative to the wall decreases to zero due to the high adverse pressure gradient, flow separation is developed. Preventing possible separation requires resisting to high adverse pressure in the boundary layer. Thus, engineers use vortex creators for such situations to increase boundary layer energy. The main purpose of using

vortex generator is creating different size of vortices which occur between enhanced high energy flow at the edges of the boundary layer and low energy flow in the remaining part of the boundary layer.

Adverse pressure gradient takes place when $dp/ds > 0$ which causes the flow velocity u to decrease along s . If the magnitude of the adverse pressure gradient is high enough the flow velocity can go to zero.

$$u \frac{du}{ds} = -\frac{1}{\rho} \frac{dp}{ds} + \nu \frac{\partial^2 u}{\partial y^2}$$

where s and y are streamwise and normal coordinate paths.

Abrupt changes in surface shapes can cause occurrence of the vortices due to variation in the pressure. They are also important to determine the created vortices paths and they follow the surface of the aircraft. Vortices which have greater size have higher velocity components and may cause undesirable increase in drag by hitting other parts of the aircraft. Furthermore; interactions between vortices may cause variation in size and should be taken into consideration.

Drag force mainly can be divided into viscous and pressure components. Viscous force component arises from the interaction between the fluid and the skin of the body; and directly related to the area of the surface of the body that is in contact with the fluid. However, main purpose of this study is not dealing with the viscous force component. The aim is to decrease pressure drag component by modifying the vortices behaviors. Variation in the strength and path of vortices can change the low and high pressure fields around the aircraft and can directly change the pressure drag component. Instead of one strong vortex, more than one but weaker vortices may cause decrease in the pressure drag component.

$$V = \frac{K}{2\pi r}$$

K corresponds to the vortex strength and r is the distance of the point from the vortex core. Induced velocity at any point depends on the vortex size and the distance of the point from the core. Moreover, it should be noted that the induced velocity at any point can be found by superimposing the effects of the all vortex cores.

The easiest and most economical way of modeling turbulent flows is using RANS equations. The Spalart-Allmaras model is a simple one-equation model which solves a modeled transport equation for the turbulent viscosity. Spalart-Allmaras turbulent model gives relatively good results for boundary layers subjected to adverse pressure gradients.

Turbulence production has been found only where vortices are generated near walls in wall-bounded flows. However, one should consider the effect of mean strain on the turbulence production. Reduction in the production of eddy viscosity where the vorticity size exceeds the strain rate is achieved by including rotation and strain tensors both. Eliminating one of them can cause overprediction of the eddy viscosity itself in certain circumstances.

III. VALIDATION

Computational Fluid Dynamics with RANS method was used to analyze the flow field around base C-130 aircraft. Results and method was validated with the experimental results in a study carried out by [Pinsky, Gray, Welch and Yechout, 2009]. A 1/48th scaled model of C-130, that had wings removed due to force balance limits of the test section, was used in the experiments (Figure 1-a). CAD model

that was used in the CFD analyses had been generated from the scanned model of an actual C-130E. Main wing of the aircraft was then removed for the agreement with the test model (Figure 1-b).

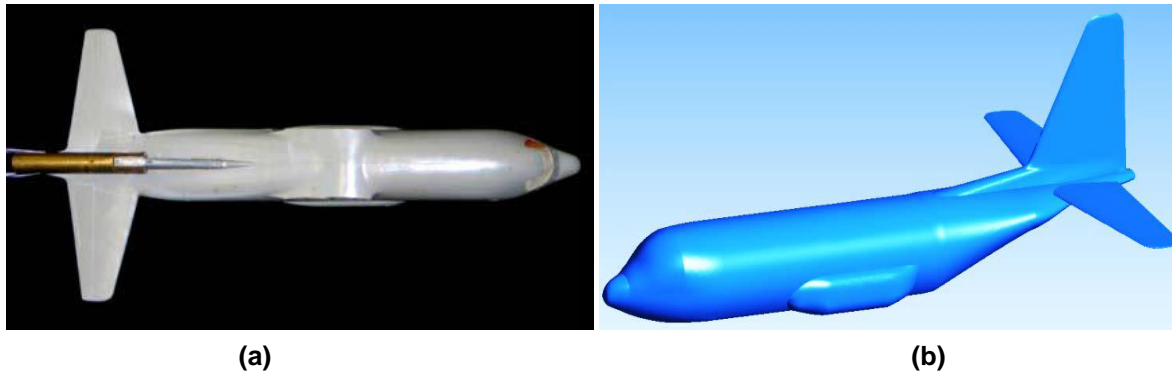


Figure 1: 1/48th scaled C-130 (a) wind tunnel test model, (b) CFD model

Experimental data includes drag coefficient values at deck angles between 0.7° and 10.7° and 0.3 Mach number. CFD analyses with different RANS turbulence models were performed at same flow conditions in the experiments to be able to determine the most suitable one for the rest of the study (Figure 2).

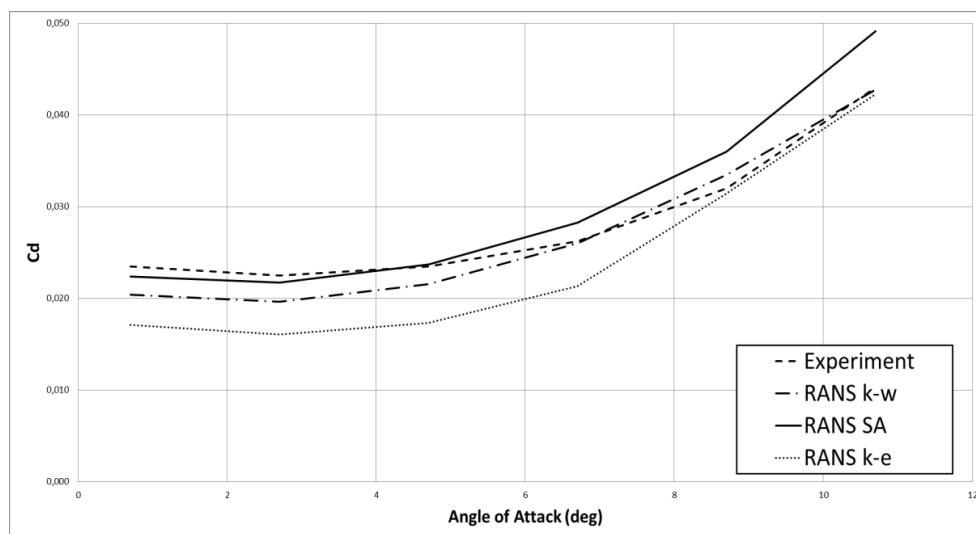


Figure 2: Validation results of the turbulence models

As discussed in references of [Mirzaei, Karimi and Vaziri, 2012; Claus, Morton, Cummings and Bury, 2005; Bergeron, Cassez and Bury, 2009; Pang, Ng and Chiu, 2013], Large Eddy Simulation (LES), Detached Eddy Simulation (DES) or Delayed Detached Eddy Simulation (DDES) would be better to analyze the whole domain more correctly; since more details of physical phenomena would be considered in turbulent flow. On the other hand, in their experimental and numerical studies on a simplified fuselage model of C-130H, [Morton, Vignes and Bury, 2006] noted that there was nearly no lift-and-drag difference between RANS and DES turbulence models even if DES was superior in portraying the vortices in the wake. Thus, due to the increasing computational cost and high number of required analyzes in the design part, RANS modeling was decided to be used and accepted as having enough accuracy at initial design part.

For the CFD simulations of the validation case, Reynolds number is 3.266×10^6 , which is similar with the Reynolds number for the 1/48th scale model used at the tests. The difference between experimental and CFD results is thought to be due to the dissimilarities between the aircraft models used. All of the turbulence models, which are suitable to be used for bluff bodies, gave acceptable results. Spalart-Allmaras and k- ω turbulence models are the closest ones. Since the aircraft operates

most of the time at $0^\circ < \alpha < 4^\circ$ cruise angles [Calarese, Crisler and Gustafson, 1985] for maximum range and endurance [Pinsky, Gray, Welch and Yechout, 2009]; the Spalart-Allmaras turbulence model which gave better results at this range angles of attack was chosen.

IV. BACKGROUND

This paper is the second part of an ongoing study to improve the performance of C-130 aircrafts serving in the Turkish Air Forces (TURAF). Since the main cargo door area is a significant contributor to the overall drag of C-130 due to vortices and possible flow separation, first part of this study focused on drag reduction of the aircraft by aft fuselage modification using finlets (Figure 3).

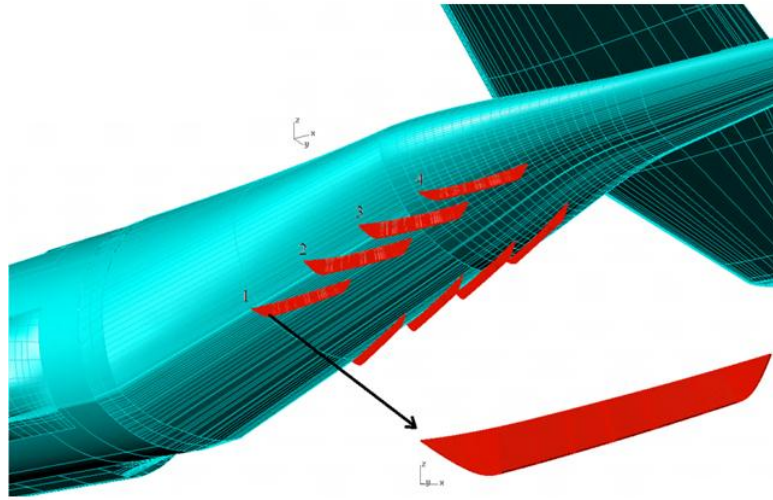


Figure 3: Finlet configuration-1 installed on underside of C-130 upswept aft fuselage

Finlets are 4 pairs of fins added to the surface of the underside of the C-130 aft fuselage. Similar to the vortex generators, finlets create small vortices that reduce production of stronger vortices at the upswept region. In addition, low energy boundary layer flow is energized by these small vortices near the edge of boundary layer. 14 different finlet configurations were analyzed in the first phase. As given in Table 1, design parameters were finlets' cross-section, length, height, thickness, leading edge sweep angle and number.

Table 1: Design parameters of the finlet configurations

	Length (m)	Height (m)	Thickness (m)	Cross- section	Divert (deg)	Sweep (deg)	Number
Conf.1	1.6	0.18	0.04	Rectangular	-	45	4 + 4
Conf.2	1.6	0.18	0.03	Rectangular	11	-	4 + 4
Conf.3	1.6	0.18	0.03	Rectangular	11	-	2 + 2
Conf.4	1.6	0.18	0.03	Rectangular	11	45	4 + 4
Conf.5	1.6	0.30	0.03	Rectangular	11	-	4 + 4
Conf.6	2.1	0.18	0.03	Rectangular	11	-	4 + 4
Conf.7	1.6	0.16	0.03	Elliptical	11	-	4 + 4
Conf.8	1.6	0.18	0.03	Elliptical	11	30	4 + 4
Conf.9	1.6	0.24	0.03	Elliptical	11	15	4 + 4
Conf.10	1.6	0.20	0.03	Elliptical	11	15	4 + 4
Conf.11	1.6	0.22	0.03	Elliptical	11	15	4 + 4
Conf.12	1.6	0.20	0.03	Elliptical	11	15	4 + 4
Conf.13	1.6	0.21	0.03	Elliptical	11	15	4 + 4
Conf.14	1.6	0.21	0.03	Elliptical	11	15	5 + 5

Since the vertical stabilizer of the aircraft does not influence the flowfield around the upswept section of the fuselage, [Bury, Morton and Charles, 2008; Bergeron, Cassez and Bury, 2009; Morton, Vignes and Bury, 2006] used a simplified, tailless C-130 geometry in their experimental and numerical studies. This simplified the meshing process and reduced the grid size. So, the CAD model of C-130 used in the validation analyses was simplified for the aftbody modification analyses by removing the vertical stabilizer.

Moreover, although the main wing provides an additional undesirable downwash on the empennage and rear section of the fuselage [Bury, Morton and Charles, 2008; Bergeron, Cassez and Bury, 2009; Morton, Vignes and Bury, 2006] had to remove the main wing from the model due to practical considerations. In the same manner, evaluation of the main wing's contribution was performed during the analyses to prevent an increase in computational cost. However, after comparison of the flowfield around aftbody of C-130, induced effect of lifting surfaces was seen as an important factor that determines vortices' behavior (Figure 4).

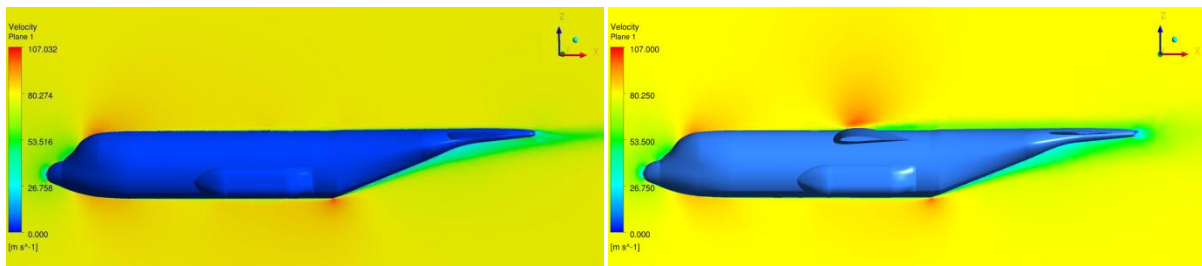


Figure 4: Velocity contours of the base configuration (a) without main wing; (b) with main wing

During the computational analyses, only a certain design parameter for each configuration was changed to understand its contribution to the drag reduction performance of the finlets. By evaluating the flowfield at the end of each analysis, design parameters of the next configuration were decided. Finally, an optimum finlet design was found with required modifications.

V. COMPUTATIONAL METHODOLOGY

The methods of grid generation and numerical setup that had been used for the first study was repeated in the second phase. Also, the same simplified CFD model of C-130 was used at the analyses. As the meshing process, unstructured triangular surface grid was generated by using GAMBIT and tetrahedral volume grid was constructed with the prism layers in between by using TGRID. In order to catch the flow vortices behavior correctly, fine grid was applied on the lower surface of the upswept aft body (Figure 5-a). Also a grading limit was defined on the surfaces of the microvanes in order to keep them fine enough during the meshing process. To be able to see the effect of the microvanes, only the grids around the microvanes were modified at each analysis by keeping the grids on the other surfaces unchanged (Figure 5-b).

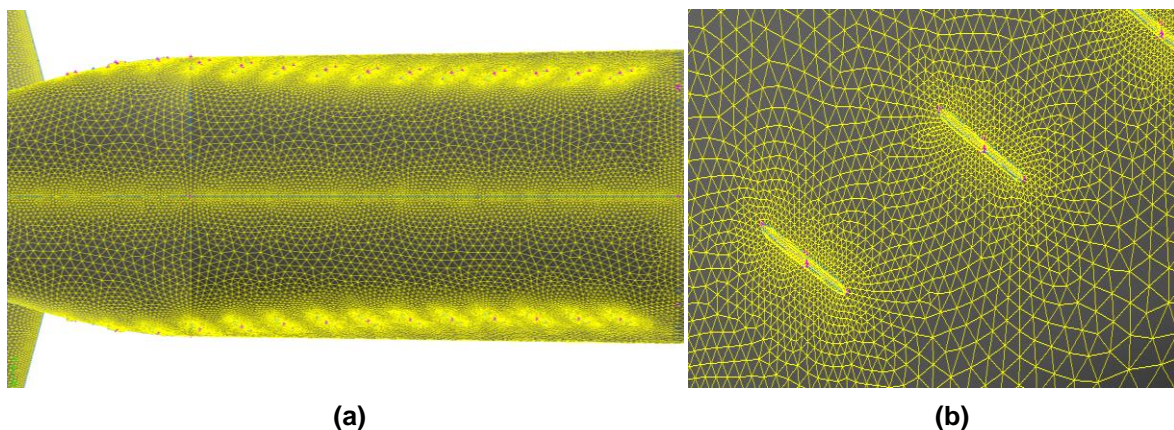


Figure 5: Surface mesh of the (a) underside of the aft fuselage; (b) microvanes

Grid convergence study was applied to the volume mesh at the wake region in order to avoid mesh dependency. Also, the fine grid region was extended to the distance which is nearly equal to five aircraft length from the tail to capture the vortex structure behind the aircraft correctly and prevent the early dissipation of it (Figure 6).

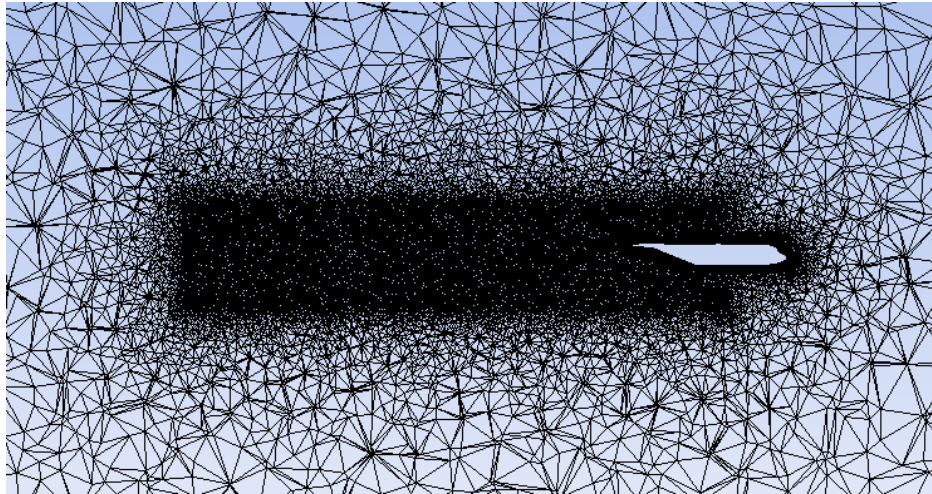


Figure 6: Distribution of the grids near wake of the aircraft

The flow domain was established as a sphere having a radius of twenty times of the body length (Figure 7). Velocity inlet boundary condition, which is suitable for incompressible analysis, was selected for the outer boundary. While actual cruise speed of C-130 aircraft is 130 m/s, free stream velocity was taken as 80 m/s at 0° flight angle of attack. Thus, analyses were performed in incompressible region with the Reynolds number of 1.16×10^8 based on the fuselage length. Compressibility was ignored to decrease computational cost by considering the accuracy losses. In design analyses, generated grid contains 25 prism layers with a geometric growth rate of 1.4 and an average y^+ value of 0.1 which is required for good resolution of the velocity gradient in the boundary layer for Spalart-Allmaras turbulence model. The final grid has minimum 10.6×10^6 cells. Grid size was increased up to 15 Million cells with grid adaption when the main wings were included.

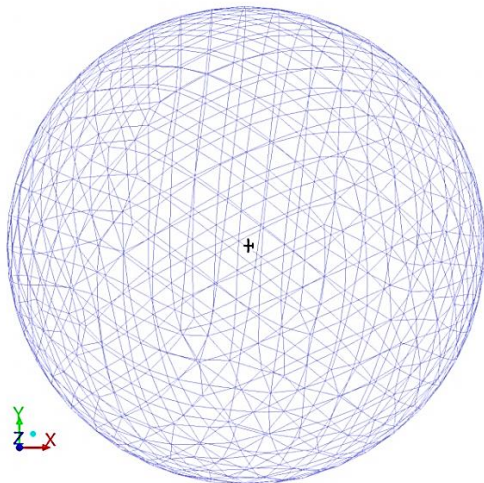


Figure 7: The outer boundary

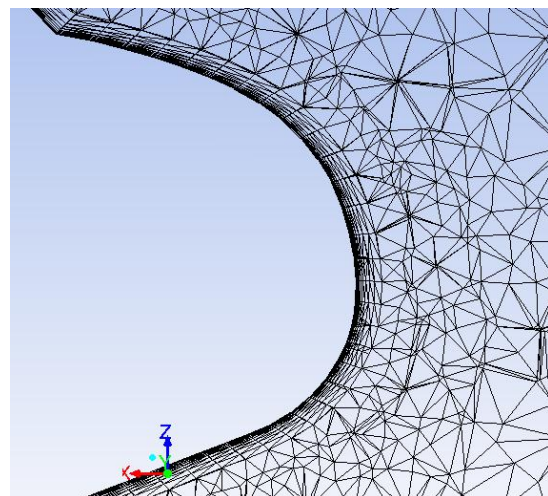


Figure 8: Boundary layer grid on the nose

ANSYS Fluent 14.0 which solves steady, three-dimensional, incompressible RANS equations were used at all analyses. Spalart-Allmaras turbulence model was chosen as the most suitable turbulence model for this type of problem with available resources. Pressure based solver was used with Green-Gauss node based gradient option. Second order pressure and momentum discretization was

performed to prevent early dissipation. The calculations were performed at the TURAF Academy Networks Laboratory on a Linux cluster. 5 nodes of that cluster were dedicated for the computations. Each node has a quad core Intel Core i7-2600K processor and 8 GB of shared memory.

VI. MICROVANE DESIGN

While finlets reduce drag significantly, they may interfere with cargo loading and airdrop operations because of their position on the main cargo door; and may also cause an adverse effect on aircraft structure due to their size and so the aerodynamic load. In addition, modeling difficulties and future problems of manufacturing caused the necessity of determining a similar but different drag reduction approach. Therefore, the drag reduction performance of microvanes was decided to be compared. Microvanes are bumped-shaped, small devices located at each side of the aircraft's aft fuselage to reduce drag. As shown in Figure 9, a plurality of microvanes having equal distances in between are located on a line starting from the breakline of the fuselage and extending through the horizontal stabilizer. Functions of microvanes and finlets are same. Both of them provide separation of big upsweep vortices into smaller ones to reduce adverse pressure gradient at the back of the aircraft and reduce the pressure drag.

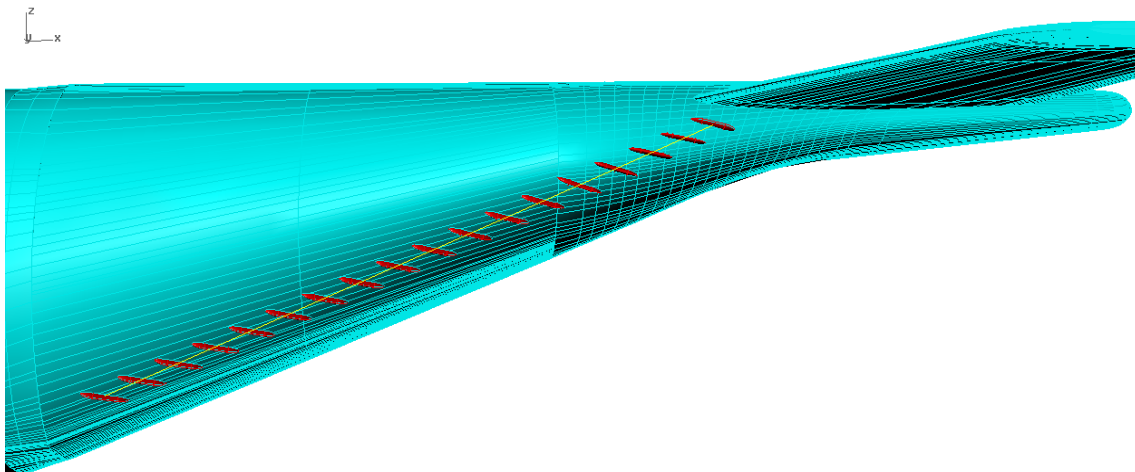


Figure 9: 18 microvanes located on a line, in equal distances

Finlets are nearly 4 or 6 times bigger than the microvanes (Figure 10). While 4 or 5 finlets at each side of the fuselage can be enough to obtain desired reduction in drag coefficient, due to their smaller size, required number of microvanes at each side may increase up to 30 to reduce drag similarly.



Figure 10: (a) A finlet design sample; (b) 1st microvane design; (c) 2nd microvane design

Sizes of two different microvanes used during the design analyses are given in Table 2. After evaluating the design parameters of initial analyses, microvane sizes were reduced by half. The final

microvane design having nearly 0.25 m of length would be considered enough to create desired performance in drag reduction.

Table 2: Microvane sizes (m)

Design	Length (m)	Height (m)	Thickness (m)
Micro#1	0.50	0.06	0.05
Micro#2	0.25	0.03	0.03

Microvanes are positioned on the fuselage such that each microvane has an incidence angle of between 30° and 60° nose up relative to the airflow. For initial analyses, all the microvanes were uniformly positioned at 30° with respect to the free stream (Figure 9). Then, looking at the behavior of the vortices and the streamlines, the incidence angles were updated by orienting each microvane with respect to the local flow direction of the air about the fuselage, at the location of the microvane. Finally, the angles of some microvanes, especially ones at the rearward, were enhanced for better performance. Figure 11 shows the updated and then the enhanced placement of microvanes of the similar configuration.

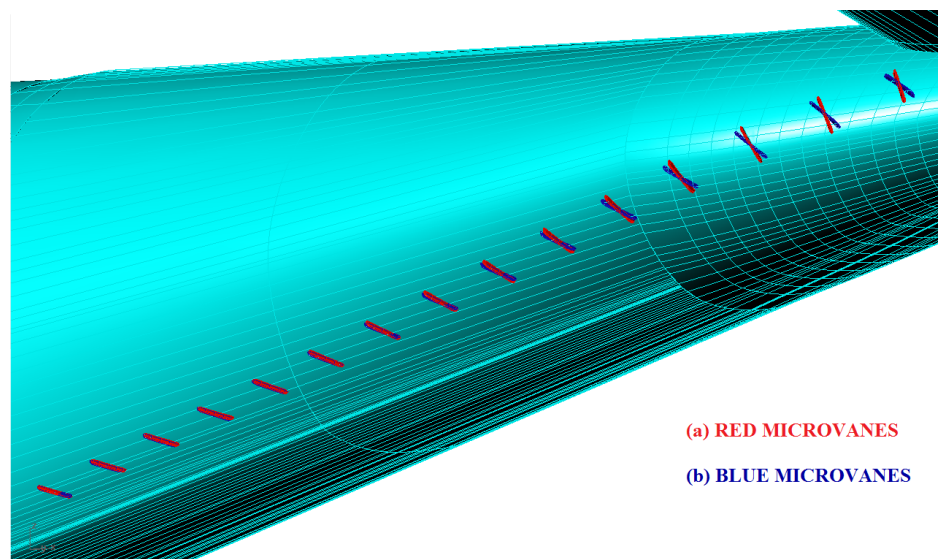


Figure 11: 15 microvanes positioned (a) with respect to the streamlines; (b) then enhanced

The microvane configurations analyzed in this study are shown in Table 3. Initial analysis was performed without wing to reduce the grid size. However, it was decided to add main wing due to its induced effect on vortices. In these first two configurations, 18 drag reduction elements of the bigger microvane design were used. Then the size of the microvane was reduced half, and the number of the microvanes was varied between 10 and 30 to find the optimum value.

Table 3: Microvane Configurations

Conf.	Design	Number	Incidence	Wing
1	Micro#1	18+18	All has 30°	no
2	Micro#1	18+18	All has 30°	yes
3	Micro#2	15+15	Updated considering streamlines	yes
4	Micro#2	15+15	Enhanced	yes
5	Micro#2	20+20	Enhanced	yes
6	Micro#2	10+10	Enhanced	yes
7	Micro#2	25+25	Enhanced	yes
8	Micro#2	30+30	Enhanced	yes

VII. RESULTS & CONCLUSION

In this section, effects of microvanes on C-130 aircraft are discussed, and the results are briefly compared with the previous finlet study. As mentioned earlier, CFD analyses were performed with Spalart-Allmaras turbulence model. Generated grids were tried to be kept unchanged to eliminate mesh dependency factor on results. In order to evaluate the behavior of vortices, different turbulence models with various initial grid spacing had been used for comparison. X-vorticity iso-surface comparison of Spalart-Allmaras with $y^+ < 1$ and k-epsilon with $y^+ > 30$ are shown in Figure 12 (a) and (b) respectively. Flow fields for two types of turbulence models are similar and that eliminates detail analyses of different turbulence models in terms of vortices' behaviors.

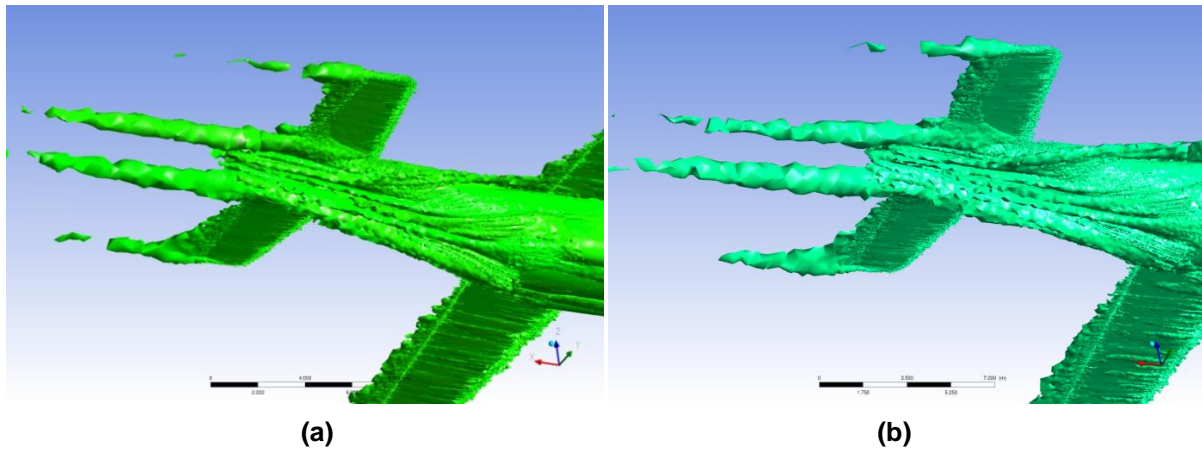


Figure 12: X-vorticity iso-surface of (a) Spalart-Allmaras; (b) k-epsilon turbulence models

Figure 13 shows the streamlines around base and modified C-130 configurations respectively. At both configurations; airflow generally follows the longitudinal axis of the fuselage up to the aft section. At the upswept section, the flow changes direction, and forms a pair of streamwise vortices. For the base aircraft, the circulation of the vortices increases with the additional vortices. Increasing circulation causes an undesired situation by increasing local velocity and decreasing local pressure. However, with the help of the microvanes, vortices stay separated. So, local velocities and the size of the low pressure field decrease.

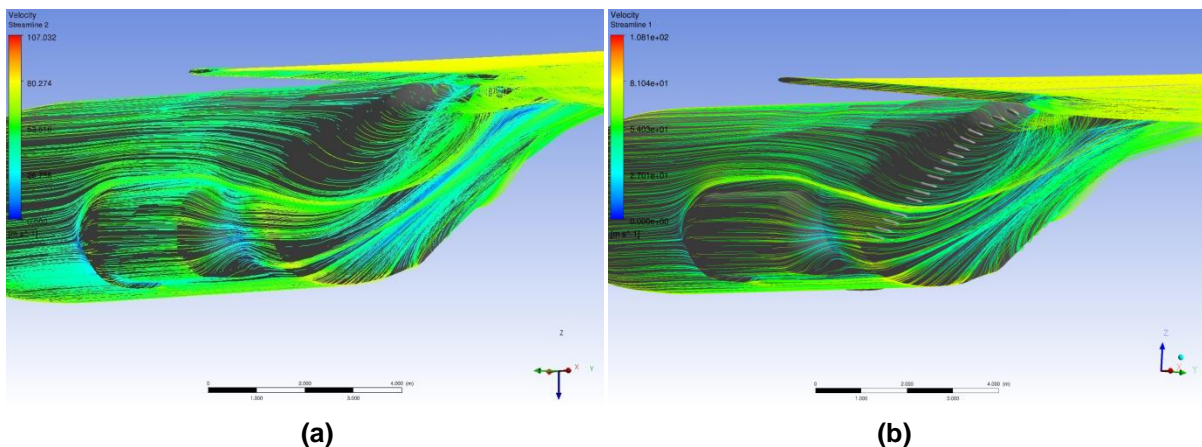


Figure 13: Streamlines around C-130 (a) base model; (b) with microvanes

For the base and the modified aircraft, cross-planes of x-vorticity along the aft section of fuselage are compared in Figure 14. The difference between two configurations is outstanding. The size of the upsweep vortices can be clearly seen at the base configuration. The vortices become stronger as they progress downstream and interact with the tail. On the other hand, working as a group, microvanes reduce the strength and size of the vortices by preventing them to combine into bigger vortices.

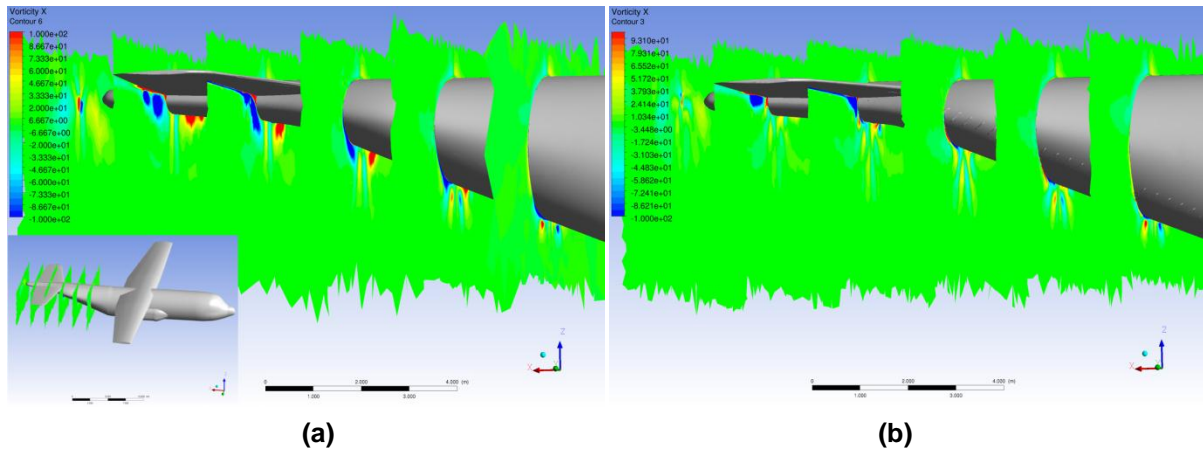


Figure 14: X-vorticity cross-sections (a) for base aircraft; (b) for microvane configuration

Decreased low pressure field due to the microvanes can be seen in the pressure contours that are given in Figure 15. Magnitude of the lowest pressure at the back of the aircraft increased up to mid-range values and a uniform distribution is achieved. As it is discussed in theory part; pressure component of drag force is calculated by the net pressure force evaluation on aircraft. Increase in the pressure at the back of the aircraft helps balancing of the high pressure field in front of the aircraft. Unnecessary increase in local velocities causes energy loss and increase in fuel consumption.

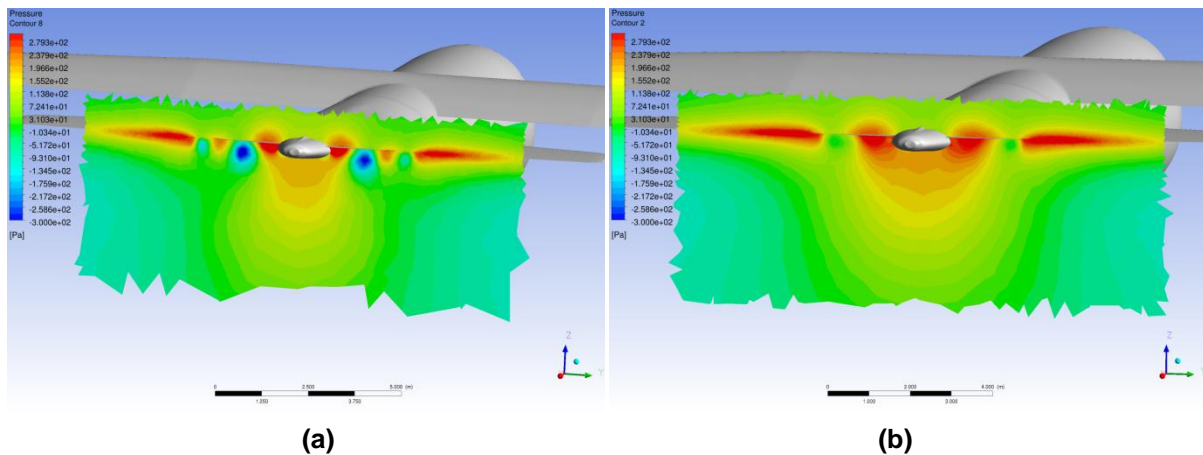


Figure 15: Pressure contour at the trailing edge of tail (a) for base C-130; (b) with microvanes

Drag reduction values of each microvane configuration are given in Table 4. Considering 1 drag count as 0.0001 of drag coefficient, around 18 drag counts of reduction is achieved with the addition of microvanes in Configuration 7. As mentioned in the design part, size of the first microvane design was reduced by half in the second design. It is seen that; reducing the size of microvanes increases the drag reduction performance of them. Frictional force is directly proportional to the surface area of the microvanes. Thus, decrease in drag coefficient after Configuration 2 is due to the reduction in frictional forces. Therefore, smaller-sized microvanes were preferred for the rest of the configurations.

Results also show that attitude of the microvanes affects their performance. At initial analyses, same incidence angle was given for all microvanes. After having evaluated the streamlines during post-process studies, some of the microvanes' incidence angles were updated depending on their locations. Then these angles were enhanced and additional decrease in drag coefficient was achieved.

As it is seen from Table 4, the most important factor to reach the highest reduction performance is the optimum number of the microvanes attached on each side of the aft fuselage. From 10 to 30 units of microvanes per side were used in the analyses. The configuration having 25 microvanes at each side

of the aftbody has been found as the most optimum one. Additional microvanes caused increase in the drag coefficient by increasing the frictional force.

Table 4: Drag reduction results of microvane configurations

Conf.	Design	Number	Incidence	Wing	Drag Count*
1	Micro#1	18+18	All has 30°	no	4.70
2	Micro#1	18+18	All has 30°	yes	6.65
3	Micro#2	15+15	Updated	yes	10.00
4	Micro#2	15+15	Enhanced	yes	16.20
5	Micro#2	20+20	Enhanced	yes	16.70
6	Micro#2	10+10	Enhanced	yes	12.60
7	Micro#2	25+25	Enhanced	yes	18.40
8	Micro#2	30+30	Enhanced	yes	15.90

*1 drag count is equal to 0.0001 unit of reduction in aircraft's drag coefficient.

At the first phase, analyses showed that, cross-section properties and total number of finlets are important design parameters. Finally, 15.7 drag count of reduction was achieved with the optimum finlet design. On the other hand, by the microvane approach, drag reduction is increased up to 18.4. Moreover; modeling, manufacturing and mounting these smaller add-ons are easier and more practical.

For the aircrafts having highly swept aftbody, such as cargo transport aircrafts with a rear cargo door, microvanes lead to decrease drag associated with upswept section of the fuselage. More than 4 % reduction of the total aircraft drag is achieved with microvanes. Achievement in drag reduction causes big possession when the total number of cargo flights of a fleet and the fuel costs are considered.

Stability variations due to usage of microvanes were also taken into consideration. When results were evaluated, it was seen that variation in pitch moment coefficient can be regarded as negligible due to the symmetry. On the other hand, small variation in yaw and roll moment coefficients was detected. However, while maneuvering, with small changes in deflection angles of control surfaces, this variation can be compensated. Furthermore, if the weight issue is taken into consideration, additional 25 microvanes at each side of the airplane will require an increase of less than 0.1% in total aircraft weight.

At further studies, drag reduction potential of microvanes will be investigated at various angles of attack. DES & DDES or LES may also be performed for chosen configurations to reach more accurate results.

References

- Bury, Y., Morton, S.A. and Charles, R. (2008) *Experimental investigation of the flowfield in the close wake of a simplified C-130 shape; A model approach of airflow influence on airdrop*, 26th AIAA Applied Aerodynamics Conference, AIAA 2008-6415, Jan 2008.
- Epstein, R.J., Carbonaro, M.C. and Caudron, F. (1994) *Experimental investigation of the flowfield about an upswept afterbody*, J. of Aircraft, Vol. 31, No. 6, p: 1281-1290, Nov-Dec 1994.
- Thomas, A.S.W. (1985) *Aircraft drag reduction technology - A summary*, AGARD Rept. 723: Aircraft Drag Prediction and Reduction, North Atlantic Treaty Organization, p: 1.1-1.20, Jul 1985.
- Quass, B., Howard, F.G., Weinstein, L.M. and Bushnell, D.M. (1981) *Longitudinal grooves for bluff body drag reduction*, AIAA 81-4095, Vol.19, p: 535-537, Apr 1981.

- Howard, F.G. and Goodman, W.L. (1985) *Axisymmetric bluff-body drag reduction through geometrical modification*, J. of Aircraft, Vol. 22, No. 6, p: 516-522, 1985.
- Calarese, W., Crisler, W.P. and Gustafson, G.L. (1985) *Afterbody drag reduction by vortex generators*, 23rd AIAA Aerospace Sciences Meeting, AIAA 85-0354, Jan 1985.
- Wortman, W. (1999) *Reduction of fuselage form drag by vortex flows*, J. of Aircraft, Vol. 36, No. 3, p: 501-506, May-Jun 1999.
- Wooten, J.D. and Yechout, T.R. (2008) *Wind tunnel evaluation of C-130 drag reduction strakes and in-flight loading prediction*, 46th AIAA Aerospace Sciences Meeting and Exhibit, AIAA 2008-348, Jan 2008.
- Pinsky, H.G., Gray, M.C., Welch, M.D. and Yechout, T.R. (2009) *Evaluation of the drag reduction potential and static stability changes of C-130 aft body strakes*, U.S. Air Force T&E Days, AIAA 2009-1721, Feb 2009.
- Mirzaei, M., Karimi, M.H. and Vaziri, M.A. (2012) *An investigation of a tactical cargo aircraft aft body drag reduction based on CFD analysis and wind tunnel tests*, Aerospace Science and Technology, Vol. 23, p: 263-269, 2012.
- Claus, M.P., Morton, S.A., Cummings, R.M. and Bury, Y. (2005) *DES turbulence modeling on the C-130: Comparison between computational and experimental results*, 43rd AIAA Aerospace Sciences Meeting and Exhibit, AIAA 2005-884, Jan 2005.
- Bergeron, K., Cassez, J.F. and Bury, Y. (2009) *Computational investigation of the upsweep flow field for a simplified C-130 shape*, 47th AIAA Aerospace Sciences Meeting, AIAA 2009-90, Jan 2009.
- Pang, S.K.H., Ng, E.Y.K. and Chiu, W.S. (2013) *Comparison of turbulence models in near wake of transport plane C-130H fuselage*, J. of Aircraft. Vol. 50, No. 3, p: 847-852, May-Jun 2013.
- Morton, S.A., Vignes, B. and Bury, Y. (2006) *Experimental and computational results of a simplified C-130 shape depicting airflow influence on airdrop*, North Atlantic Treaty Organization, RTO-MP-AVT-133 AC/323 TP/113, 2006.